Croat Med J 2005;46(3):429-435

Volume-related Sequence of Tumor Distribution Pattern in Prostate Carcinoma: Importance of Posterior Midline Crossover in Predicting Tumor Volume, Extracapsular Extension, and Seminal Vesicle Invasion

Goran Torlakovic, Emina Torlakovic[1], Eva Skovlund[2], Jahn M. Nesland[3], Albrecht Reith[3], Havard E. Danielsen[4,5]

Department of Pathology, St. Paul's Hospital; [1]Department of Pathology, Royal University Hospital, University of Saskatchewan, Saskatoon, Canada; [2]Section of Medical Statistics; [3]Department of Pathology; [4]Department of Digital Pathology, Norwegian Radium Hospital, University of Oslo, Oslo, Norway; and [5]Division of Genomic Medicine, University of Sheffield, Sheffield, UK

Aim To evaluate intraprostatic distribution of prostate carcinoma as a function of increasing tumor size and its potential clinical relevance.

Methods Forty-six prostates with different tumor extent were three dimensionally reconstructed and analyzed with emphasis on number of separate tumors (multifocality) and its distribution on both sides of the urethral midline (laterality).

Results Three tumor distribution patterns were identified: multiple bilateral without posterior midline crossover, multiple bilateral with crossover, and single bilateral (global) tumors. Unilateral tumors were rare (2%). The pattern of tumor distribution was associated with total tumor volume, presence and volume of high grade component, presence of extracapsular extension, and seminal vesicle involvement. Bilateral tumors with crossover were larger than bilateral tumors without crossover (Spearman's $\rho = 0{,}728$, $P < 0.001$) and were associated with adverse pathological features including capsular penetration, seminal vesicle invasion, and surgical margin involvement. However, only high-grade volume was independently and highly associated with seminal vesicle involvement (OR = 2.64, 95%, CI = 1.181-5.340, $P < 0.001$). Total (OR = 2.53 [1.23-3.74], $P < 0.001$) and index tumor (OR = 2.54 [1.31-4.93], $P < 0.001$) volumes were independently associated with capsular penetration.

Conclusions The distribution of bilateral prostatic carcinomas with and without crossover may have clinical relevance because of their relation to total and high-grade volume.

In the recent years, new strategies for performance of the prostate biopsies have been proposed for the purpose of enhanced tumor detection (1-3). This shift from lesion-directed biopsy toward systematic random sampling of the prostate has emphasized the need and importance of clinically useful interpretation of topographically complex findings. Attempts were made to predict the number of separate tumors when more than one sextant site showed cancer (4) and to predict cancer volume in bilateral positive biopsies (5). The analysis of zonal distribution of the prostate cancer and, most recently, plane of the greatest cancer spread and intracompartmental distribution as a function of cancer volume were described (6,7). It is known, however, that the majority of patients with prostate carcinoma, have more than one tumor; extensively disperse growth and

multiple histological patterns can be found within a single tumor (6,8-10). Therefore, little is still known about how tumor laterality and multifocality, as identified on needle biopsy, can help to generate clinically useful prediction of the pathologic stage. Complex growth, intraprostatic distribution of the largest tumor (index tumor), and simultaneous presence of multiple incidental tumors within a single prostate make it difficult to understand the tumor extent based on the pretreatment biopsy reports. However, patterns of prostate carcinoma distribution based on the analysis of laterality and multifocality, rather than anatomic location and zonal distribution have not yet been described. Epstein et al (4) addressed the question of multifocality of the prostate cancer on sextant biopsies and found that when more than one sextant site showed cancer, there were differences in terms of whether the tumors sampled were multifocal or solitary, depending on which sites were positive. Loch et al (5) showed that contralateral biopsies did not contribute to prediction nor distinguish bilateral spread from contralateral incidental cancer.

In this study, we performed a systematic analysis of multifocality and laterality of prostate adenocarcinomas in 46 three-dimensionally (3-D) reconstructed prostates from preoperatively untreated patients with tumors of variable size. Based on the combination of multifocality and laterality of the tumors, we identified volume-related patterns of prostate carcinoma distribution which could provide a prediction of capsular perforation and seminal vesicle invasion. Our results suggest that prostate sampling at the posterior midline may provide clinically useful staging information in the pretreatment evaluation of prostate cancer patients.

Subject and Methods

We morphologically analyzed 194 completely embedded prostates from previously untreated men with prostatic adenocarcinoma, who underwent radical retropubic prostatectomy between 1988 and 1996 at the Norwegian Radium Hospital, Oslo, Norway. None of these patients had preoperative morphologic evidence of regional lymph node metastases. Patients age varied from 54 to 73 years (median 63.5). All procedures in tissue collection were in accordance with regional ethical standards outlined by the hospital Ethics Committee.

The prostates were submitted for morphological examination *in toto*. Careful tracing under microscopic examination was done on each glass slide in all 194 specimens, creating a tumor outline by a marker pen. Representative cases for three dimensional reconstruction were selected from 194 specimens, in order to determine the number of tumor foci and the tumor distribution in the prostate. To follow the changes in tumor distribution with tumor growth, the percentage of slides containing tumor was used to select 46 cases to be representative of small, medium, and large size tumors. We included 16 cases with 1-33%, 15 cases with 34-66%, and 15 cases with 67-100% slides involved by the tumor.

The following features were also recorded for each case: 1) all Gleason grades (9) in all tumor foci on each slide; 2) tumor extension beyond the limits of the prostate (capsular penetration); 3) resection margin involvement; 4) seminal vesicle involvement; 5) percentage of slides containing tumor (as a measure of tumor dispersion within the prostate); 6) laterality of the tumor; and 7) zonal distribution.

Three-dimensional Reconstruction

Three-dimensional prostate models were created from transparent copies made from all tissue glass slides with previously outlined cancer areas. First, copies of the tissue slides belonging to the same transverse level were matched and pasted together. Subsequently, serial levels were pasted sequentially into a real prostate model. The distance between individual transparent levels corresponding to the thickness of a single tissue slice was left empty. The left and right halves of the gland were then aligned one toward the other by matching tissue contours (Fig. 1).

Number of Tumors

The number of tumors in each prostate was determined after three dimensional reconstruction. In the absence of overlap, the carcinoma area was considered part of the same tumor if the distance to the nearest adjacent focus was within 3 mm in any of the three dimensions of the model. All tumors within the same prostate were recorded in numerical order, based on the calculated percent involvement with a number 1 (T1) designating the index tumor.

Tumor Percentage and Tumor Volume

Each distinct prostate tumor and its high-grade component (Gleason grades 4 and 5) were evaluated (9). Calculation of the percent of prostate tumor involvement was based on measurements performed as previously described, using the grid method (11-13). Tumor volume was calculated from tumor mass and the density of the prostate tissue.

Laterality of the Tumor

For all reconstructed prostates, the exact anatomic location of each tumor was recorded. The total tumor volume was measured with the grid-

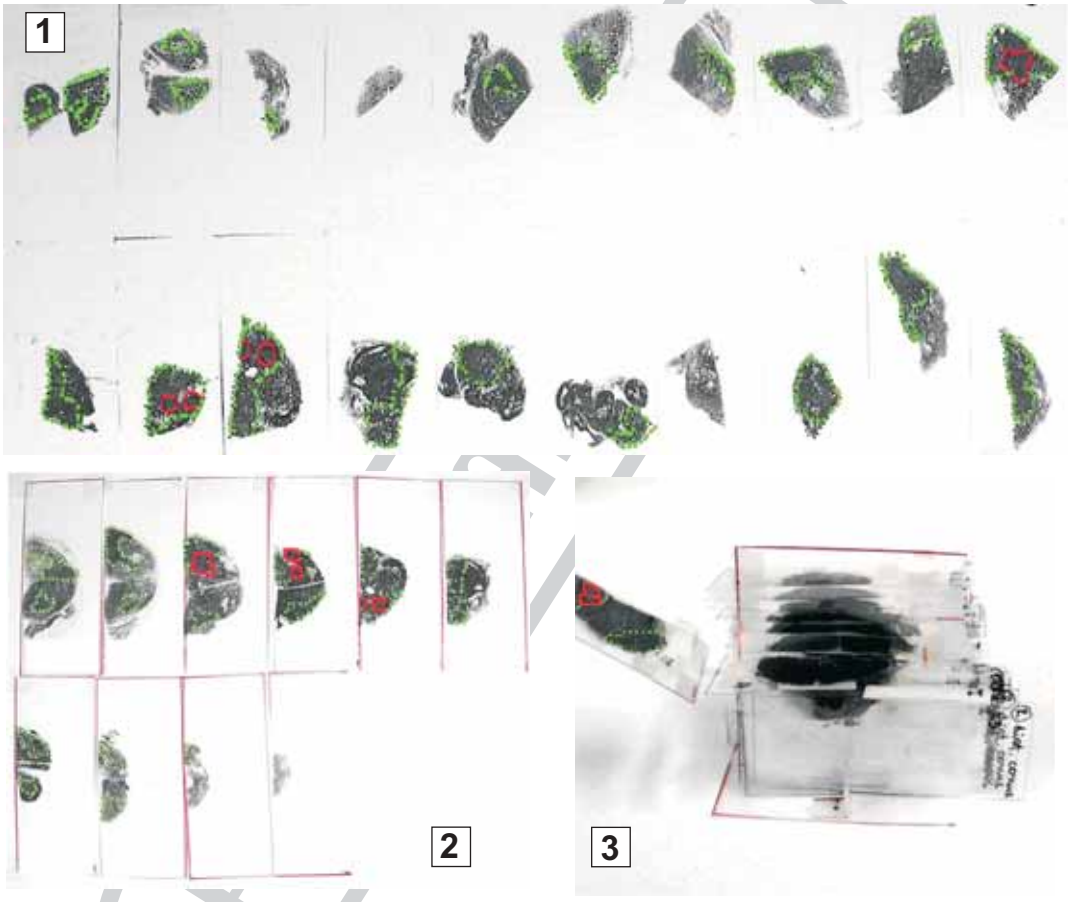

Figure 1. Three steps in three-dimensional reconstruction of the prostate from routine sections, using plastic transparent slides. The end result is a plastic transparent model, which can be held in hand and provides easy and reproducible assessment of tumor distribution. The presence of the tumor in the histology section is outlined by dots (for total tumor) and full lines (for high-grade tumor).

Table 1. Association among the pattern of prostate tumor distribution and total tumor volume, high-grade volume, and prostate tumor (pT) category

Pattern of tumor distribution	No. (%)	Total tumor volume (mL; median, range)*	No. (%) of high-grade†	High-grade volume (mL; median, range)*	No. of tumors with pT category‡		
					pT1-2	pT3a§	pT3b§
Multiple unilateral	1	0.37	1	0.27	1	0	0
Multiple bilateral without crossover	17	2.66 (0.06-4.52)	6	0.47 (0.24-2.07)	9	8	1
Multiple bilateral with crossover	12	3.06 (1.35-8.30)	11	1.78 (0.22-3.93)	3	9	2
Single bilateral (global)	16	10.85 (3.27-38.73)	16	3.75 (0.07-31.84)	1	15	8
Total	46	4.63 (0.06-38.73)	33	1.85 (0.07-31.84)	13	32	11

*$P<0.001$ (Spearman correlation, $\rho=0.74$ for total tumor volume and $\rho=0.68$ for high-grade volume).
†According to Gleason (9).
‡pT1-2 – confined, pT3a – extracapsular extension, unilateral of bilateral, pT3b – seminal vesicle involvement (21).
§$P=0.006$ for extracapsular extension and $P=0.004$ for seminal vesicle involvement (Spearman correlation $\rho=0.34$ for extracapsular extension and $\rho=0.42$ for seminal vesicle involvement).

method for each side separately. For our study, the "midline" of the peripheral zone was defined by inspection of 3D-reconstructed specimens, using the urethra as a primary anatomic reference point. Tumors with continuous growth across posterior urethral midline (crossover) were recorded. The exact extent of the tumor with continuous growth over the midline on each side of the specimen (left and right) was measured with the grid method. The tumors were designated as "midline tumors" if fulfilling previously published criteria (ie less than 10% difference between the 2 lobes) (5).

Statistical Analysis

Associations between categorical variables were analyzed by the χ^2-test. Spearman correlation was used where appropriate. The simultaneous effect of several (explanatory) variables was analyzed by multivariable regression models. When the dependent variable was continuous or ordinal, multiple linear regression was applied. For binary dependent variables, logistic regression was used. *P*-values below 0.05 were considered statistically significant. The regression models were reduced by backward elimination to include the significant variable only. SPSS 12.0 (SPSS Inc, Chicago, IL, USA) software was used for statistical analysis.

Results

The weight of the prostates varied from 13 to 76 g (median 45). Pathological stage is included in the Table 1. A total of 110 tumors were identified in 46 prostatectomy specimens. The smallest total tumor volume was 0.06 mL and the largest 38.73 mL (median 4.63 mL). The volume of the total tumor (Spearman's $\rho = -0.629$, $\rho = -0.616$, $P = 0.001$), and percentage of prostate involvement (Spearman's $\rho = -0.723$, $P < 0.001$) all showed an inverse relation with the number of tumors. All prostates with tumor involvement of more than 20% or with tumor volume larger than 8.5 mL had only one bilateral/global tumor. The smallest global tumor was 3.27 mL.

Tumor distribution patterns changed with the increasing total tumor volume. The smallest tumors were multiple, with bilateral prostate involvement. With increasing volume, the following changes in the distribution pattern were seen: from multiple bilateral without crossover to multiple bilateral with crossover, and finally to an extensive single bilateral tumor (global tumor). There was only a single prostate with 0.37 mL multifocal, unilateral tumor (Table 1).

The presence of index tumor (T1) crossover (Fig. 2) was associated with increasing tumor volume (Spearman's $\rho = 0.728$, $P < 0.001$), percentage of prostate involved by the tumor

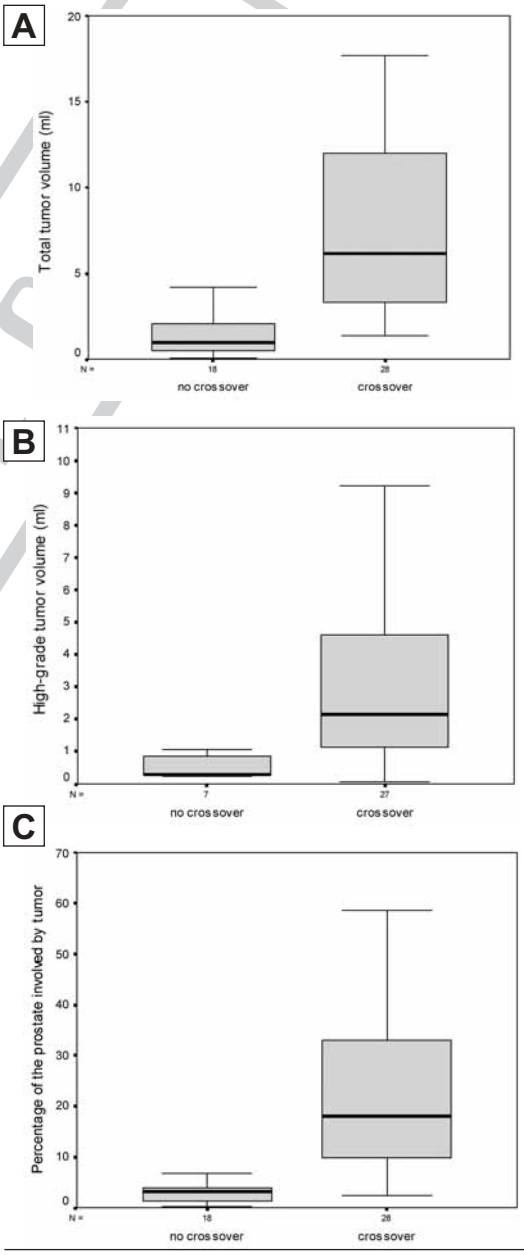

Figure 2. Prostate carcinomas with posterior crossover are much larger than those without crossover. Box-and-whiskers plots for: (**A**) differences for total tumor volume, (**B**) volume of a high-grade component, and (**C**) percentage of the prostate involved by the tumor.

(Spearman's $\rho = 0.733$, $P < 0.001$) and T1 volume (Spearman's $\rho = 0.768$, $P < 0.001$), as well as percent of prostate involved by T1 (Spearman's $\rho = 0.748$, $P < 0.001$). Only one index tumor was classified as "midline tumor" (equally distributed between left and right lobe) with volume of 5.3 mL. No incidental "midline tumors" were found.

The occurrence of high-grade tumor component appeared to increase exponentially and was present in all prostates with total tumor volume larger than 2 mL. The volume of the high-grade tumor component was proportional to the volume of the total tumor (Spearman's $\rho = 0.619$, $P < 0.001$) and volume of the index tumor (T1) (Spearman's $\rho = 0.643$, $P < 0.001$).

A significant correlation was found between the Gleason sum and total tumor volume (Spearman's $\rho = 0.299$, $P = 0.043$) and also with the index tumor (T1) volume (Spearman's $\rho = 0.306$, $P = 0.039$), but not with the percentage of prostate involved by the tumor.

Only the largest (index tumor, T1) showed capsular penetration. The capsular penetration was significantly associated with several parameters of tumor extent when these were analyzed individually (total tumor volume, $P < 0.001$, OR = 2.53 95% CI = 1.23-3.74), T1 volume ($P < 0.001$, OR = 2.54 [1.31-4.93]), percentage of prostate involved by the tumor ($P = 0.003$, OR = 3.57 [1.52-8.34]), and percentage of prostate involved by T1 ($P = 0.004$, OR = 3.61 [1.50-8.74]). However, regression analysis showed that it was only the total tumor volume and T1 volume, which were independently associated with capsular penetration. Also, half of the tumors penetrated the capsule before they crossed the posterior urethral midline.

Only the index tumor (T1) involved the seminal vesicles. The analysis showed that the seminal vesicle involvement was significantly associated with the Gleason sum ($P = 0.003$, OR = 3.85 [1.60-9.27]), total tumor volume ($P = 0.023$, OR = 5.91 [1.64-21.33]), high grade tumor volume ($P < 0.001$, OR = 2.64 [1.18-5.34]), percentage of prostate with tumor involvement ($P = 0.003$, OR = 2.43 [1.35-4.38]), T1 volume ($P = 0.014$, OR = 3.39 [1.29-8.98]), and percentage of prostate involved by T1 ($P = 0.003$, OR = 1.07 [1.02-1.12]) when these were analyzed individually. However, regression analysis of all of these parameters revealed that it was only the high-grade tumor volume ($P = 0.04$, OR = 2.06 [1.11-5.55]) that was significantly associated with the seminal vesicle involvement. Of 11 prostates without high-grade component, none had seminal vesicle invasion. In patients with total tumor volume ≤4.5 mL, only 4% had seminal vesicle involvement, but as many as 50% had seminal vesicle involvement when total tumor volume was >4.5 mL.

Peripheral zone tumors extending into the transition zone were significantly larger ($\chi^2_1 = 5.477$, $P = 0.009$) than those with capsular penetration alone.

Discussion

The results of our study provide a link between the patterns of multifocality and laterality of the tumor with the tumor volume, intraprostatic distribution, capsular penetration, and seminal vesicle invasion. Based on the current needle biopsy strategies, it is not possible to distinguish bilateral spread from contralateral incidental cancers of the prostate or predict pathologic stage (5,14). The volume of the tumor, including high-grade volume, is not known preoperatively and only exceptionally, in rare centers, it is available postoperatively. Few studies of the relationship between volume and intraprostatic zonal and anatomical distribution of carcinoma of the prostate are available (6-8). In our approach to the analysis of tumor distribution, we did not focus on the anatomic or zonal spread of the adenocarcinoma, but rather on the significance of the multifocality, laterality, and index tumor crossover as a function of an increasing total tumor volume.

Our study showed that prostate carcinoma is already a multifocal and bilateral disease at very low volume (<0.5 mL), which is in agreement with several previous studies (8-10,15,16). Remarkably, the tumors were already global when the percentage of prostate involvement reached between 15% and 20%. This probably reflects the fact that prostate tumors have a tendency for disperse growth and that their growth is limited to a certain point by a transition zone boundary (17,18). Transition zone boundary was also confirmed in our study by showing that the tumors that penetrated the capsule were significantly smaller than those that penetrated the transition zone boundary. Also, about half of the tumors in our study penetrated the capsule before they crossed

the posterior urethral midline. In our study, all penetrating tumors were index tumors, whereas Ruiter et al (9) reported that about 25% of the tumors with capsular penetration in multifocal disease were not index tumors. Our findings concur with the recent conclusion by McNeal and Haillot (7) that patterns of spread of adenocarcinoma of the prostate are not entirely random and unpredictable, but are guided in part by the complex stromal organization of the gland.

The laterality of the tumor (unilateral vs bilateral) was considered to be a potential prognostic factor of prostate carcinoma (19). Byar and Mostofi (8) reported that as much as 80% of the prostates with adenocarcinoma had bilateral involvement. In our study, 98% of the prostates had bilateral involvement by carcinoma, in both the smaller 3-D reconstructed sample of 46 prostates and the large sample of 194 prostates (results not shown). Loch et al (20) found that 48% of index tumors were bilateral, which is similar to 59% in our study. The most important finding of our study was that 92% of tumors with crossover had high-grade component, whereas high-grade component was found in only 35% of the tumors without crossover. These findings suggest, similar to the findings of Chan et al (2,10), that finding of a tumor in a posterior midline biopsy could give additional clinical information. In their study, this additional information refers to an increased chance of detecting a prostate cancer after negative sextant biopsies. In our study, this additional information refers to an ability to demonstrate higher probability of a larger tumor volume and higher probability of capsular penetration, as well as seminal vesicle invasion. An important previous work by Chan et al (2), who created detailed maps of tumor foci, showed that the posterior midline peripheral zone is generally not involved in tumors <0.5 mL, rarely in tumors between 0.5 mL and 2.0 mL, and often in tumors >2.0 mL, which is in agreement with our findings. Hence, study by Chan et al (2) and our study indicate that the presence of a tumor in the posterior midline on the needle biopsy may be suggestive of a large bilateral index tumor.

Since our study and the study by Loch et al (20) showed that the presence of tumor bilaterality alone without reference to the index tumor crossover has no relevance for staging, we suggest that the presence of posterior crossover should be further studied as a potential prognostic factor in prostate cancer.

In conclusion, with increasing total tumor volume, there is a sequential change in the pattern of tumor distribution from multifocal, bilateral disease without crossover, through multifocal bilateral disease with index tumor crossover, to a single bilateral tumor (global tumor). The presence of the largest tumor crossover was positively associated with pT category. Finding of the index tumor crossover in the posterior midline needle biopsy should be considered as potentially informative for pretreatment staging as for now.

References

1 Hodge KK, McNeal JE, Terris MK, Stamey TA. Random systematic versus directed ultrasound guided transrectal core biopsies of the prostate. J Urol. 1989;142:71-4.

2 Chen ME, Troncoso P, Johnston DA, Tang K, Babaian RJ. Optimization of prostate biopsy strategy using computer based analysis. J Urol. 1997;158:2168-75.

3 Eskew LA, Bare RL, McCullough DL. Systematic 5 region prostate biopsy is superior to sextant method for diagnosing carcinoma of the prostate. J Urol. 1997;157: 199-202.

4 Epstein JI, Lecksell K, Carter HB. Prostate cancer sampled on sextant needle biopsy: significance of cancer on multiple cores from different areas of the prostate. Urology. 1999;54:291-4.

5 Loch T, McNeal JE, Stamey TA. Interpretation of bilateral positive biopsies in prostate cancer. J Urol. 1995; 154:1078-83.

6 McNeal JE, Redwine EA, Freiha FS, Stamey TA. Zonal distribution of prostatic adenocarcinoma. Correlation with histologic pattern and direction of spread. Am J Surg Pathol. 1988;12:897-906.

7 McNeal JE, Haillot O. Patterns of spread of adenocarcinoma in the prostate as related to cancer volume. Prostate. 2001;49:48-57.

8 Byar DP, Mostofi FK. Carcinoma of the prostate: prognostic evaluation of certain pathologic features in 208 radical prostatectomies. Examined by the step-section technique. Cancer. 1972;30:5-13.

9 Ruijter ET, van de Kaa CA, Schalken JA, Debruyne FM, Ruiter DJ. Histological grade heterogeneity in multifocal prostate cancer. Biological and clinical implications. J Pathol. 1996;180:295-9.

10 Chen ME, Johnston DA, Tang K, Babaian RJ, Troncoso P. Detailed mapping of prostate carcinoma foci: biopsy strategy implications. Cancer. 2000;89:1800-9.

11 Humphrey PA, Vollmer RT. Intraglandular tumor extent and prognosis in prostatic carcinoma: application of a grid method to prostatectomy specimens. Hum Pathol. 1990;21:799-804.

12 Qian J, Wollan P, Bostwick DG. The extent and multicentricity of high-grade prostatic intraepithelial neoplasia in clinically localized prostatic adenocarcinoma. Hum Pathol. 1997;28:143-8.

13 Bostwick DG, Shan A, Qian J, Darson M, Maihle NJ, Jenkins RB, et al. Independent origin of multiple foci of prostatic intraepithelial neoplasia: comparison with matched foci of prostate carcinoma. Cancer. 1998;83: 1995-2002.

14 Humphrey PA, Walther PJ. Adenocarcinoma of the prostate. Part II: Tissue prognosticators. Am J Clin Pathol. 1993;100:256-69.

15 Miller GJ, Cygan JM. Morphology of prostate cancer: the effects of multifocality on histological grade, tumor volume and capsule penetration. J Urol. 1994;152(5 Pt 2):1709-13.

16 Sesterhenn IA, Mostofi FK, Mattrey RR, Sands JP, Davis CJ Jr, McCarthy WF. Preliminary results of three-dimensional reconstruction of previously imaged prostates. Prostate Suppl. 1992;4:33-41.

17 McNeal JE. Anatomy of the prostate and morphogenesis of BPH. In: Kimball FA, editor. New approaches to the study of benign prostatic hyperplasia. New York: Alan R. Liss, Inc.; 1984. p. 27-53.

18 McNeal JE. Cancer volume and site of origin of adenocarcinoma in the prostate: relationship to local and distant spread. Hum Pathol. 1992;23:258-66.

19 Graham SD Jr, Bostwick DG, Hoisaeter A, Abrahamsson P, Algaba F, di Sant'Agnese A, et al. Report of the Committee on Staging and Pathology. Cancer. 1992; 70(1 Suppl):359-61.

20 Loch T, McNeal JE, Stamey TA. Interpretation of bilateral positive biopsies in prostate cancer. J Urol. 1995; 154:1078-83.

21 Fleming ID, Cooper JS, Henson DE, Hutter RV, Kennedy BJ, Murphy GP, et al, editors. AJCC cancer staging manual. 5th ed. Philadelphia (PA): Lippincott-Raven; 1997. p. 219–24.

Received: November 22, 2004
Accepted: March 30, 2005

Correspondence to:
Emina Emilia Torlakovic
Department of Pathology
Royal University Hospital
College of Medicine
University of Saskatchewan
103 Hospital Drive
Saskatoon, SK S7N 0W8, Canada
emt323@mail.usask.ca